Statistics of polymer chains near a notch and consequences for twin polymer single crystals

Marc L. Mansfield
Michigan Molecular Institute, 1910 W St Andrews Road, Midland, Michigan 48640, USA
(Received 26 September 1988; accepted 30 December 1988)

It has been argued that flaws exist in the standard nucleation theory of polymer crystal growth because this theory seems to predict that the notches observed in twin crystals of polyethylene should fill out so rapidly as not to be observable. However, I argue that the observed growth in the notch is reconcilable with standard nucleation theory. When proper consideration is taken for the ability of polymer chains to diffuse into the notch, the observed nucleation rates are not surprising. I consider four separate cases. In the first case, I assume that polymers, although attracted by the growth front, are not attracted strongly enough to be adsorbed prior to crystallization. In the second case, I assume that polymers adsorb readily on the crystal face, and then crystallize very near the point of first contact. In the third case, I assume that chains adsorb on the growth front prior to crystallization and that they are able to diffuse about on the growth front through large distances prior to crystallization. In the fourth case, polymers adsorb rather weakly, and reversibly, attaching and reattaching a number of times prior to crystallization. I am able to rule out the second case, while all the others predict a lower than expected nucleation rate and also predict the observed molecular weight and temperature trends.

(Keywords: nucleation theory; crystal growth; nucleation rates)

INTRODUCTION

Twin polyethylene single crystals are known to grow from dilute solution. A range of structures can be observed depending on such things as crystallization temperature, but under certain conditions, structures such as the one shown in *Figure 1* are observed. Sadler and co-workers[1,2] discuss the structures that are formed as a function of both crystallization temperature and molecular weight. The notches present on such crystals, such as the one formed by the intersection of the $(\bar{1}10)$ and the (110) planes in *Figure 1* are of particular interest. As Sadler and co-workers[1,2] have pointed out, the standard nucleation theory of polymer crystallization[3] is hard put to explain the existence of these notches. The reason for this is most obvious in *Figure 2*, which displays the crystal structure in the vicinity of such a notch. As can be seen in *Figure 2*, site A is expected to be a very active site for the addition of new polymer stems because a new stem can be added with no additional surface area. This is to be contrasted with addition away from the notch, such as at site B, which requires creation of new crystal surface. Addition at sites such as site B in *Figure 2* is deemed, in the standard nucleation theory[3], to require surmounting a large nucleation barrier, while the nucleation barrier for site A should either be non-existent or very small.

On the basis of the above statements, one would argue that such notches should not be observed at all because any that did exist would rapidly fill out. Such notches do exhibit enhanced growth, but at nothing like the rate one would expect on the basis of standard nucleation theory[1,2]. This paper presents an explanation of the growth of these crystals (including temperature and molecular weight trends) without abandoning the standard nucleation model. A number of other papers from this institute address the issue of curved crystals[4–10].

The observed nucleation rates in the notch decrease with either increasing molecular weight or increasing temperature[1,2]. A complete explanation would require me to explain not only the lower than expected nucleation rates, but the observed temperature and molecular weight trends as well.

Nucleation rates in the notch prove to be smaller than expected because the notch is not directly accessible. Because of gaps in the understanding of polymer crystallization, I find it necessary to consider a number of separate cases. These are considered individually in the following sections. This paper calls upon a rather large number of mathematical models and computer simulations to support its contentions. To avoid distraction from the central theme of the paper, these are all relegated to a number of appendices.

CASE A

In this section I consider the case of weak attraction between dissolved chains and the crystal growth front. Chains in the vicinity of a weakly attracting flat wall are repelled by the wall. This fact is discussed in Appendix 1. Chains near walls have less entropy than those in bulk solution. Unless the attraction is sufficiently strong, the attractive energy will not compensate for the decrease in entropy and the wall will repel the polymer. As the attraction strength increases, the chains undergo a transition to adsorption. This transition is not abrupt, so the definition of the position of the transition is rather vague. The definition adopted here is the point at which

0032-3861/89/091623-10$03.00

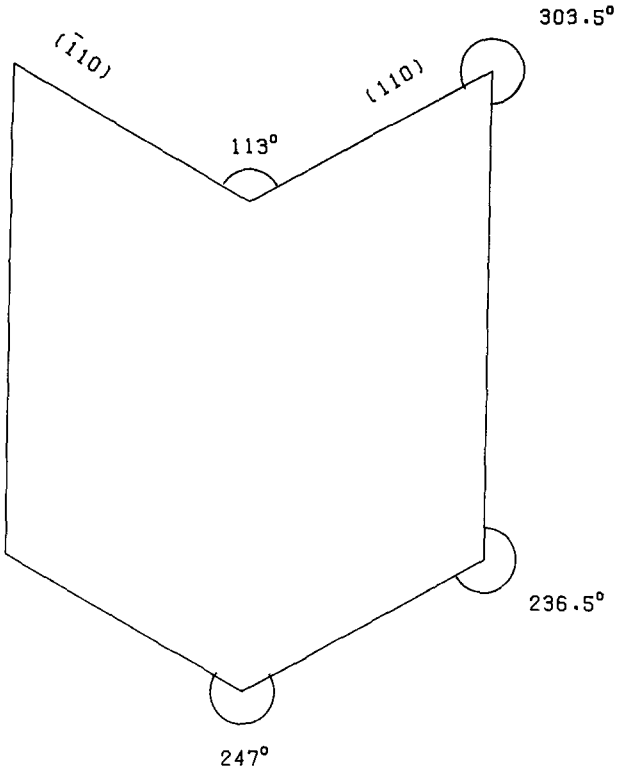

Figure 1 Typical structure of the polyethylene twin crystals

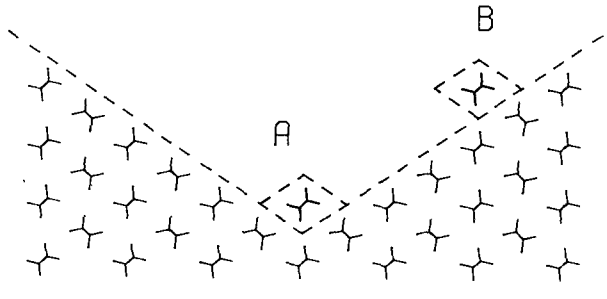

Figure 2 Nucleation in the notch (site A) is expected to occur much more rapidly than on a flat surface (site B) because no new surface is created during nucleation in the notch

the partition function of chains near the wall equals the partition function of chains distant from the wall. Appendix 4 calculates the position of the adsorption transition for the chain model introduced in Appendix 3.

In this section, I consider the case in which the attraction between dissolved polymer and the growth front is so weak that dissolved chains are repelled by the growth front. This case is contrary to the generally accepted belief that polymers adsorb on the crystal face prior to crystallization. Note however, that there are no compelling reasons why the adsorption temperature should coincide or be correlated with the dissolution temperature because the one concerns polymers at interfaces while the other concerns polymers in bulk phases. If chains are repelled by the growth front, then the repulsion between chain and crystal represents an entropic contribution to the nucleation barrier. Chains probably do adsorb prior to crystallization, but I choose here to also consider this less likely possibility.

Appendices 2 and 3 consider the statistics of ideal chains near notches formed as the intersection of two semi-infinite planes. These appendices indicate that polymers are repelled more strongly by a notch than by a flat plane if they are on the desorption side of the adsorption transition. This is to be expected because the chain loses even more entropy near a notch than near a flat wall. Conversely, on the adsorption side of the transition, polymers are preferentially attracted by the notch. Either effect, adsorption or repulsion, becomes more pronounced with increasing molecular weight.

With the assumption that polymer chains are repelled by the growth front, these results predict a lower than expected nucleation rate within the notch. They are also consistent with the observed molecular weight and temperature trends because the repulsion of the notch becomes stronger with either increasing molecular weight or temperature.

CASE B

In this section I consider the case in which the attraction between dissolved chains and the growth front is strong enough that polymers adsorb prior to crystallization, and that they both adsorb and crystallize at sites very near the point of first contact between the chain and the crystal.

The results of Appendices 5–8 firmly establish that Brownian particles make first contact in notches or with wedges with a probability density proportional to $d^{(\pi/2-\alpha)}$ for α the angle subtended by the notch ($\alpha<\pi/2$) or wedge ($\alpha>\pi/2$) and with d the distance from the vertex. Thus, the probability density vanishes at $d=0$ for a notch, and diverges at $d=0$ for a wedge. Consequently, we predict that most polymer chains diffusing up to the crystal make first contact with the crystal at site near the horns, and that first contacts in the vicinity of the notch are very infrequent (see Appendix 8.)

Appendices 5–8 treat diffusing polymers as structureless Brownian particles, and lead to the assertion that probabilities of first contact scale as $d^{0.593}$ near the notch, becoming very small as d decreases. I am, of course, concerned with nucleation occurring at one particular lattice site over length scales of a few Å (site A in *Figure 2*) and therefore cannot neglect the internal structure of the chain. The power law $d^{0.593}$ undoubtedly holds over length scales d such that $R_g \ll d \ll C$, for R_g the bulk solution radius of gyration and C the macroscopic dimension of the crystal. Very near the notch, at length scales $d \ll R_g$ and comparable to lattice dimensions, I expect the first contact probability to be even smaller than the power law expression.

Appendices 5–8 predict a highly non-uniform first-contact probability. Therefore, the case examined here, crystallization near sites of first contact, is untenable because the crystal growth front is uniform. This only allows two other possibilities. Under cases of strong adsorption, the chains must become adsorbed at the site of first contact, then diffuse along the surface before crystallizing. In the case of somewhat weaker adsorption (but not so weak that case A above applies) the chains may or may not adsorb near the point of first contact, and may adsorb and desorb several times before finally crystallizing. These cases are examined in the next two sections.

CASE C

In this case, I assume that polymers are attracted strongly

by the crystal, so strongly that they adsorb irreversibly at or near the site of first contact between the polymer and the crystal, and that they subsequently diffuse about on the crystal before crystallizing. As pointed out above, the assumption of surface diffusion prior to crystallization is necessary because the growth front is uniform while the distribution of first contacts is very non-uniform. The chains probably diffuse about on the surface until they find either a niche or until they nucleate at some other site. First contact is very probable near the horns of the crystal, but very improbable near the notch. Therefore, chains which crystallize in the notch must diffuse into the notch from long distances, without nucleating at any other sites. This probably accounts, at least in part, for the smaller than expected nucleation rates in the notch.

The notch attracts the chain more strongly than a flat wall, as indicated by the results of Appendix 3. The strength of this attraction increases with decreasing temperature, and this temperature dependence most probably accounts for the observed temperature dependence of notch nucleation. Surface diffusion must certainly decrease with increasing molecular weight, accounting for the molecular weight trends observed. Barring any strong temperature dependence of the surface diffusivities permits me to explain both molecular weight and temperature trends.

CASE D

In this case I assume that the attraction between the chain and the growth front is somewhat weaker, so that adsorption does not necessarily occur at the point of first contact, or is not necessarily irreversible. However, I am assuming that adsorption does occur prior to crystallization.

In this case, contacts with the notch will still be preceded by a number of contacts at other sites (subsequent to the moment of first contact which only rarely occurs in the notch). Notch nucleation is still hampered by transport into the notch. The arguments given above for case C probably still apply.

SUMMARY AND DISCUSSION

I have considered a number of separate cases in an effort to understand the failure of chains to nucleate rapidly in the notch of polyethylene. Case A is characterized by a weak attraction between dissolved polymers and the growth front, so weak that adsorption prior to crystallization is not expected. Cases B and C are both characterized by strong attraction with irreversible adsorption immmediately after first contact. Case B is further characterized by the assumption that crystallization also occurs near the point of first contact, while case C assumes surface diffusion of adsorbed chains prior to crystallization. Case B proves to be unacceptable (first contact distributions are very non-uniform.) Case D is the case of intermediate attraction, characterized by adsorption prior to crystallization, but adsorption which is either reversible or which does not necessarily occur at the point of first contact. Of the three acceptable cases (A, C, and D), case C most closely corresponds to the current paradigm of polymer crystallization, but it is notable that in all three cases, I am able to explain the smaller than expected notch nucleation rates and the temperature and molecular weight dependence of these rates.

The problem is one of accessibility of the notch. The notch is indeed a site of very favourable nucleation, but chains cannot nucleate in the notch until they arrive there. In case A, chains are excluded from the notch by their own entropy, in cases C and D by inefficient transport.

Another possibility suggested to the author by Professor J. D. Hoffman, which I have not discussed prior to this point, also exists. Chains in the vicinity of the notch (especially at high molecular weight) may simultaneously nucleate on both flat faces, leaving a non-crystalline chain segment spanning the notch and poisoning the notch to any subsequent nucleation. This occurrence might also be responsible for the lack of nucleation in the notch.

ACKNOWLEDGEMENTS

The author thanks Professor J. D. Hoffman for suggesting this research and for a number of stimulating discussions. This research was supported in part by a grant from the National Science Foundation, Grant DMR-8607708.

REFERENCES

1 Sadler, D. M. *Polymer Comm.* 1984, **25**, 196
2 Sadler, D. M., Barber, M., Lark, G. and Hill, M. J. *Polymer* 1986, **27**, 25
3 Hoffman, J. D., Davis, G. T. and Lauritzen, J. I. Jr. in 'Treatise on Solid State Chemistry', Vol. 3 (Ed. N. B. Hannay), Plenum Press, New York (1976)
4 Sadler, D. M. and Gilmer G. H. *Polymer* 1984, **25**, 1446
5 Sadler, D. M. *Polymer Comm.* 1986, **27**, 149
6 Sadler, D. M. *J. Polym. Sci., Polym. Phys. Edn.* 1985, **23**, 1533
7 Sadler, D. M. and Gilmer, G. H. *Phys. Rev. Lett.* 1986, **56**, 2708
8 Sadler, D. M. *Polymer* 1987, **28**, 1440
9 Mansfield, M. L. *Polymer* in press
10 Hoffman, J. D. and Miller, R. L. in preparation
11 DiMarzio, E. A. and Rubin, R. J. *J. Chem. Phys.* 1971, **55**, 4318 and references therein
12 Lauritzen, J. I. and DiMarzio, E. A. *J. Ref. Nat. Bur. Stand.* 1978, **83**, 381
13 deGennes, P. G. *Scaling Concepts in Polymer Physics* Cornell University Press, Ithica, NY, 1979, p. 246–250
14 Muthukumar, M. private comunication
15 Carslaw, H. S. and Jaeger, J. C. 'Conduction of Heat in Solids', 2nd edn. Oxford University Press, Oxford (1959)
16 Abramowitz, M. and Stegen, I. A. (Eds.) 'Handbook of Mathematical Functions' Dover, New York, 1965, p. 505
17 Abramowitz, M. and Stegen, I. A. (Eds.) 'Handbook of Mathematical Functions' Dover, New York, 1965, p. 255
18 Gradshteyn, I. S. and Ryzhik, I. M. 'Table of Integrals, Series, and Products', Academic Press, New York, 1980, p. 38
19 Flory, P. J. Statistical Mechanics of Chain Molecules, Wiley, New York, 1969, p. 40
20 Abramowitz, M. and Stegen, I. A. (Eds.) 'Handbook of Mathematical Functions' Dover, New York, 1965, p. 40
21 Jackson, J. D. 'Classical Electrodynamics' Wiley, New York, 1975, p. 77

APPENDIX 1

Ideal chains near a flat wall

This is a well-known problem, discussed, for example, by DiMarzio and Rubin[11]. The case in which the wall shows no attraction or repulsion for the polymer is most easily treated as the solution of the diffusion equation[13,14]

$$\frac{\delta w}{\delta t} = D\nabla^2 W \qquad (1)$$

subject to the following boundary conditions: $W=0$ at the wall, which is taken to be the $z=0$ plane; and $W(r, t=0)=\delta(r_0-r)$, for δ the Dirac delta function and for r_0 the position of one end of the chain. In this formalism, $W(r, r_0, t)$ represents the statistical weight of chains having one end at r_0 and the other at r, and having t backbone bonds total. The Green's function of equation (1) in the absence of boundaries is, of course,

$$(4\pi Dt)^{-3/2} \exp[-(r-r_0)^2/(4Dt)] \tag{2}$$

The solution with the boundary condition $W=0$ at $z=0$ can then be easily written down by the method of images, with a source at (x_0, y_0, z_0), and a sink at $(x_0, y_0, -z_0)$:

$$W=(4\pi Dt)^{-3/2}\left\{\exp\left[\frac{-(x-x_0)^2-(y-y_0)^2-(z-z_0)^2}{4Dt}\right]\right.$$
$$\left.-\exp\left[\frac{-(x-x_0)^2-(y-y_0)^2-(z+z_0)^2}{4Dt}\right]\right\} \tag{3}$$

The quantity

$$P(r_0, t)=\int dr\, W(r_0, r, t) \tag{4}$$

represents the statistical weight of all chains with one end at r_0. The integral with W given by equation (3) is straightforward. I obtain

$$P(z_0, t)=\mathrm{erf}[z_0/2(Dt)^{1/2}] \tag{5}$$

$P(z_0, t)$ is zero at $z_0=0$, and increases monotonically to 1 at values of $z_0 \gg (Dt)^{1/2}$. Note that $(Dt)^{1/2}$ is the radius of gyration that the chain would have in bulk solution, distant from any boundaries. This predicts a depletion layer near the wall, of thickness comparable to the radius of gyration of the chain. Chains avoid the wall because their configurational entropy decreases near the wall.

The same differential equation techniques can be employed in the case that the polymer chain is attracted by the wall. This problem has been studied by DiMarzio and Rubin[11] and by Muthukumar[14]. I omit details and only point out that a depletion zone still exists in the case of weak attraction. Adsorption does not occur until the interaction becomes sufficiently strong. To adsorb on a wall, a chain must give up a great deal of configurational entropy. If the energy decrease experienced upon adsorption is not large enough, the chain will tend to avoid the wall.

APPENDIX 2

Ideal chains near a non-attracting notch

This problem requires solution of equation (1) in cylindrical coordinates (ρ, θ, z) subject to the boundary conditions $W=0$ at $\theta=\pm\alpha/2$ and $W\to\delta(r_0-r)$ as $t\to 0$, where α is the dihedral angle between the two planes forming the notch. *Figure 3* displays the coordinate system employed. The solution for these boundary conditions is given by Carslaw and Jaeger[15] while Lauritzen and DiMarzio[12] consider the special case $\theta_0=0$. The solution is

$$W=4\alpha^{-1}\pi^{-1/2}\tau^{-3/2} \exp[-\tau^{-1}(z^2+\rho^2+\rho_0^2)]$$
$$\times \sum_{n=1}^{\infty} I_s(2\rho\rho_0/\tau)\times \sin[s(\theta+\alpha/2)]\, \sin[s(\theta_0+\alpha/2)] \tag{6}$$

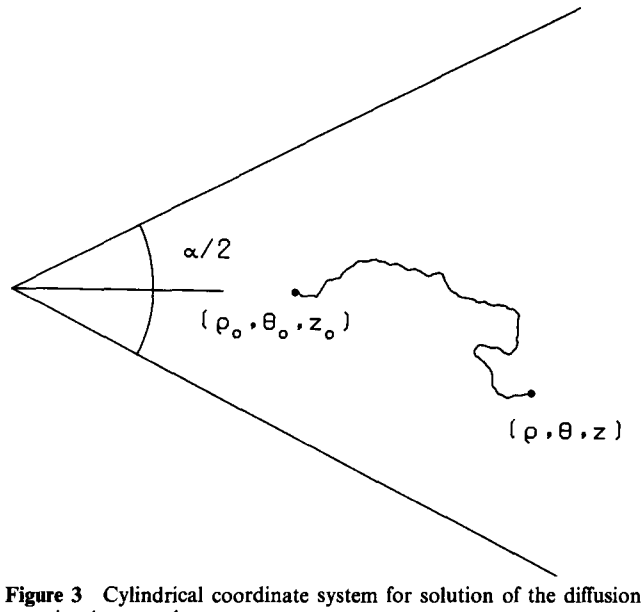

Figure 3 Cylindrical coordinate system for solution of the diffusion equation in a notch

where $\tau=4Dt$ and $s=n\pi/\alpha$. Lauritzen and DiMarzio[12] perform the integral given in equation (4) for the special case of $\theta_0=0$. Integration of W with general θ_0, equation (6), proves to be no more difficult, and so is not detailed here. The result is:

$$P(\theta_0, \rho_0)=4\pi^{-1}\tau^{1/2}\rho_0^{-1} \exp(-\rho_0^2/2\tau) \sum_{n=0}^{\infty} \frac{(-1)^n}{(2n+1)}$$
$$\frac{\Gamma(v+1)}{\Gamma(2v+1)}\cos(2v\theta_0)\times M_{-1/2,v}(\rho_0^2/\tau) \tag{7}$$

where $v=(2n+1)\pi/(2\alpha)$, and $M_{-1/2,v}$ represents one of the Whittaker functions[16]. The Whittaker functions can also be written[16] in terms of one of the confluent hypergeometric functions, $M(a, b, x)$:

$$M_{-1/2,v}(x)=e^{-x}x^{v+1/2}M(1+v, 1+2v, x) \tag{8}$$

The confluent hypergeometric functions also obey the following relationships[16]:

$$M(1+v, 1+2v, x)=e^x M(v, 1+2v, -x) \tag{9}$$

$$M(v, 1+2v, -x)=\frac{\Gamma(2v+1)}{\Gamma(v+1)\Gamma(v)}\int_0^1 e^{-xp}p^{v-1}(1-p)^v dp \tag{10}$$

Combining all the above permits me to write

$$P(\theta_0, \rho_0)=(2/\alpha)\sum_{n=0}^{\infty}\frac{(-1)^n}{\Gamma(v+1)}\cos(2v\theta_0)x^{2v}$$
$$\times\int_0^1 F(x^2, p, v)\, dp \tag{11}$$

where $x^2=\rho_0^2\tau$ and

$$F(x^2, p, v)=e^{-x^2p}p^{v-1}(1-p)^v \tag{12}$$

I may also write $x=\rho_0/2R_g$ for R_g the radius of gyration of the chain in bulk solution.

Consider the limit $\rho_0\to\infty$. In that limit, x in equation (12) becomes large, so that the factor $\exp(-x^2p)$ is non-negligible only for very small values of p. In that case we can neglect the factor $(1-p)^v$ in equation (12), it becomes arbitrarily close to unity for all non-negligible

values of the integrand as $\rho_0 \to \infty$. This permits me to use the following integral representation[17] of the gamma function:

$$z^{\nu} \int_0^{\infty} e^{-zp} p^{\nu-1} dp = \Gamma(\nu) \tag{13}$$

to obtain the series

$$\lim_{\rho_0 \to \infty} P(\theta_0, \rho_0) = 4\pi^{-1} \sum_{n=0}^{\infty} \frac{(-1)^n}{(2n+1)} \cos(2\nu\theta_0) = 1 \tag{14}$$

the sum in equation (14) being known[18].

Values of $P(\theta_0, \rho_0)$ were computed according to equation (11), with the integral over F performed numerically. When $0 < \nu < 1$, $F(x^2, p, \nu)$ has a singularity at $p = 0$, diverging as $p^{\nu-1}$. To perform the integration under such circumstances, we write

$$F(x^2, p, \nu) = f(x^2, p, \nu) + p^{\nu-1}$$

the above serving as a definition of the function f. The function f has no singularity and can be easily integrated by Simpson's rule, for example. The integral of $p^{\nu-1}$ is just $1/\nu$.

Results are plotted in the form of contour plots shown in *Figures 4* and *5* for $\alpha = 113°$, a value appropriate for polyethylene (100) twins. I should emphasize that *Figures 4*, *5*, *7*, and *8* display relative concentrations of chain ends. The overall monomer concentration was not calculated in any of the above cases. This could probably be done but it appears that it would be considerably more difficult. Until the question of whether or not polymers begin crystallizing near their ends is resolved, the distinction between monomer concentrations and chain-end concentrations should not be taken too seriously.

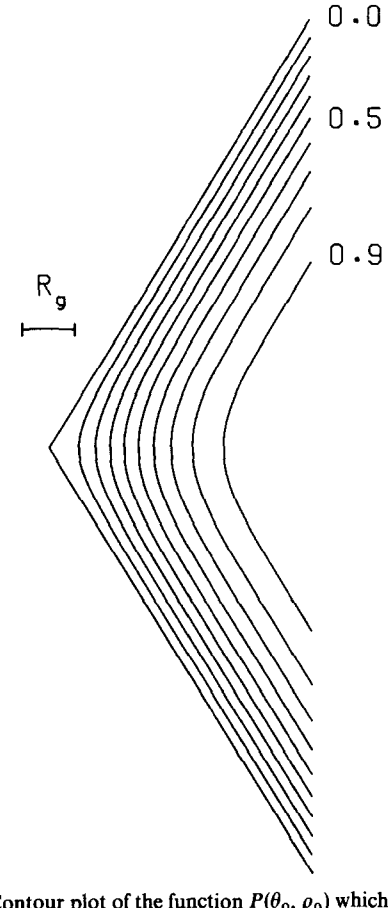

Figure 4 Contour plot of the function $P(\theta_0, \rho_0)$ which is proportional to the concentration of the ends of ideal chains in the vicinity of the notch. The length of the horizontal line equals the radius of gyration that the chain would have at sites distant from any barriers

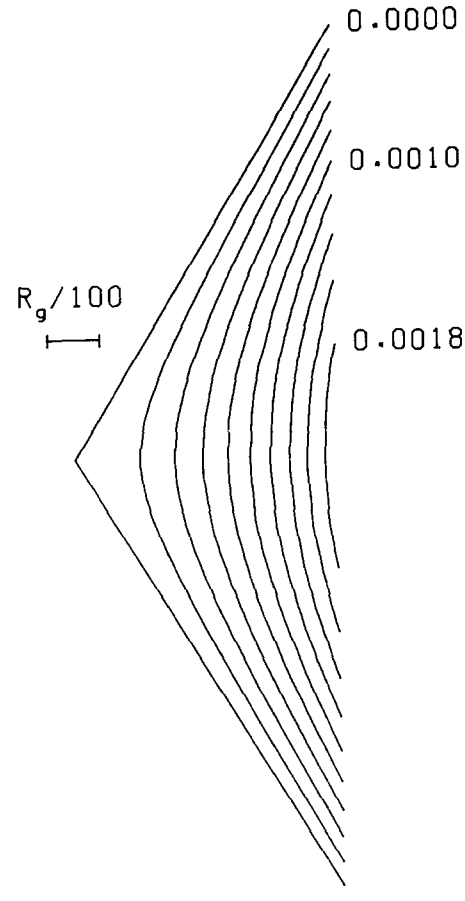

Figure 5 Same as *Figure 4*, except over a shorter length scale

The results were found to be numerically indistinguishable from the error function values given in equation (5) for sites along the wall distant from the notch, providing a check of the numerical procedure. The depletion observed near the wall becomes more severe in the vicinity of the notch. This is, of course, due to the fact that a chain near the notch experiences an even greater entropy reduction than one near a flat wall.

All dependence on ρ_0 appears in the ratio ρ_0/R_g for R_g the bulk solution gyration radius. Therefore, the depletion near the notch becomes more severe as R_g increases, as expected.

APPENDIX 3

Ideal chains near an attractive notch

This problem can also be treated by the differential equation formalism, but I expect it to be a very difficult boundary value problem and have chosen, therefore, not to make the attempt. I have been able to obtain useful results by considering a lattice model. I consider two-dimensional random walks confined to the hexagonal area shown in *Figure 6*, with the walks confined to a triangular lattice within the hexagonal region. I let M denote the number of lattice sites along one edge of the hexagon. (For clarity, *Figure 6* is drawn with $M = 10$, however, in the calculations I set $M = 100$.) When $M = 100$, there are 29 701 lattice sites. As shown in *Figure 6*, I let the letter A designate any one of the six

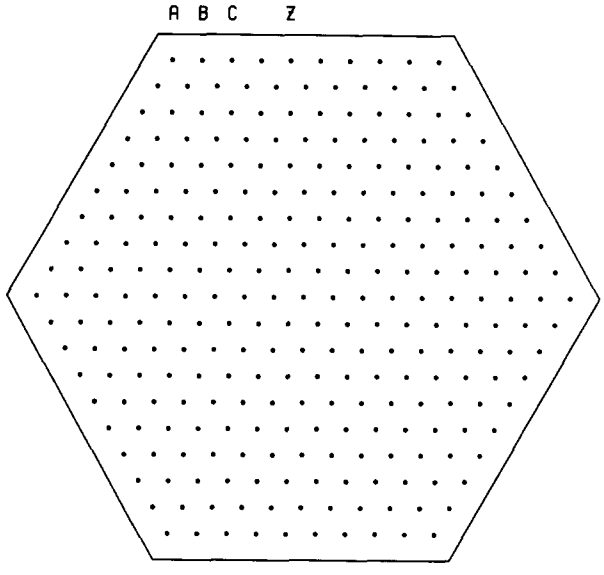

Figure 6 Schematic diagram of the lattice walk model. The six lattice sites in the corners are designated A, they contribute an energy $-2akT$ to any chain that visits them. The other sites along the walls are designated B, C, D, etc.; Z designates sites along the walls distant from both notches. The sites B, C, D, ..., Z contribute an energy $-akT$ to any chain that visits them. Sites not adjacent to any wall contribute nothing to the energy

lattice sites in the corners. I let the letter B represent any of the twelve sites along the walls immediately adjacent to the sites A. C represents sites along the walls adjacent to the B sites, etc. I let Z represent sites along the wall distant from any notch, i.e., near the middle of any wall. I consider random walks of N steps, visiting $N+1$ lattice sites. Values of N were chosen ($N=100$) so that at most a negligibly small fraction of chains in the ensemble could visit more than one notch, so that the results obtained for the enclosed domain of *Figure 6* also apply to notches bounded by semi-infinite planes. The angle subtended by the two walls, 120°, is not too far from the angle appropriate for (100) twin polyethylene crystals, about 113°. I assign an energy U_μ to the μth lattice site and define the total energy of the chain to be the sum of the U_μ values for all lattice sites visited by the chain. $U_\mu=0$ for all lattice sites except those at the boundaries. $U_\mu=-akT$ for sites along the walls except at the six lattice sites nearest the notches (the A sites in *Figure 6*), where $U_\mu=-2akT$; a is a variable parameter. Assigning a value of $-2akT$ in the corners reflects the fact that chain segments in those positions are simultaneously attracted by two walls.

The total energy of the chain which begins at site α, stepping from there to site β, from there to γ, and so forth through N steps to site ω, is, of course,

$$U_\alpha+U_\beta+U_\gamma+\ldots+U_\omega \tag{15}$$

We can also write the energy as the sum of contributions from individual steps, rather than lattice sites, if I first define

$$U_{\mu\nu}=(U_\mu+U_\nu)/2 \tag{16}$$

Then clearly, the total energy of the chain visiting sites $\alpha, \beta, \gamma, \ldots \omega$ is just

$$U_\alpha/2+U_{\alpha\beta}+U_{\beta\gamma}+\ldots+U_{\psi\omega}+U_\omega/2 \tag{17}$$

The statistical weight of this chain is

$$\exp(-U_\omega/2kT)A_{\omega\psi}\ldots A_{\gamma\beta}A_{\beta\alpha}\exp(-U_\alpha/2kT) \tag{18}$$

where $A_{\mu\nu}=\exp(-U_{\mu\nu}/kT)$. $A_{\mu\nu}$, as defined, represents the statistical weights for steps from site μ to site ν on the lattice, provided μ and ν are nearest neighbour sites. I can extend the definition to encompass all pairs of sites if I write

$$A_{\mu\nu}=\exp[-(U_\mu+U_\nu)/2kT] \tag{19a}$$

if μ and ν are nearest-neighbour lattice sites, and

$$A_{\mu\nu}=0 \tag{19b}$$

for all other pairs of sites. Equation (19b) makes explicit the fact that I do not consider steps between non-neighbouring sites.

Equation (18) represents the statistical weight of one particular walk. I can extend it to represent the statistical weight of all walks starting at the specified site α and ending at the specified site ω by summing over all possible values of $\beta, \gamma, \ldots \psi$:

$$Q_{\alpha\omega}=\textstyle\sum_\beta\sum_\gamma\ldots\sum_\psi e^{-U_\omega/2kT}A_{\omega\psi}\ldots A_{\gamma\beta}A_{\beta\alpha}e^{-U_\alpha/2kT} \tag{20}$$

Each summation in equation (20) extends over all lattice sites. If we let A represent the matrix of $A_{\mu\nu}$ values and define a column vector V_0^α whose μth element is

$$(V_0^\alpha)_\mu=\exp[-U_\alpha/2kT]\delta_{\alpha\mu} \tag{21}$$

then equation (20) becomes

$$Q_{\alpha\omega}=(V_0^\omega)^\dagger\times A^N\times V_0^\alpha \tag{22}$$

The partition function of all chains having one end at site α is defined as $Q_\alpha=\sum_\omega Q_{\alpha\omega}$ and may be written

$$Q_\alpha=W\times A^N\times V_0 \tag{23}$$

if I define the row vector W such that

$$W=\textstyle\sum_\omega(V_0^\omega)^\dagger \tag{24}$$

Defined in this way, the ωth element of W is

$$W_\omega=\exp[-U_\omega/2kT] \tag{25}$$

Calculation of Q_α would be unfeasible if I tried to store the entire A matrix in computer memory. However, this is not necessary. Note that every non-zero element of A is equal to x^0, x^1, x^2, or x^3; where $x=e^{a/2}$. Therefore, at the beginning of the calculation we can compute and store these few powers of x, and then look up the required values of $A_{\mu\nu}$ whenever they are needed. By considering the sequence of vectors defined by

$$V_{j+1}^\alpha=A\times V_j^\alpha \tag{26}$$

with V_0^α defined as in equation (21), I have

$$Q_\alpha=W\times V_N^\alpha \tag{27}$$

Therefore, I am only required to reserve enough memory to store V_j^α and V_{j+1}^α simultaneously. The elements of W can also be looked up in the table of powers of x. An additional saving is realized if in computing a particular element of V_{j+1}^α:

$$[V_{j+1}^\alpha]_\mu=\textstyle\sum_\nu A_{\mu\nu}[V_j^\alpha]_\nu \tag{28}$$

I only consider non-zero values of $A_{\mu\nu}$ and $[V_j^\alpha]_\nu$, (i.e., instead of letting ν range over all lattice sites.)

Figure 7 displays the value of $6^{-N}Q_\alpha$ as a function of a, for α a site adjacent to the wall midway between the notches, i.e., a site such as the one labelled Z in *Figure 4*. The coil dimensions of the polymer relative to the size of the hexagon are such that Q_α for $\alpha=z$ is negligibly different from Q_α for an infinite plane. In addition, 6^N is

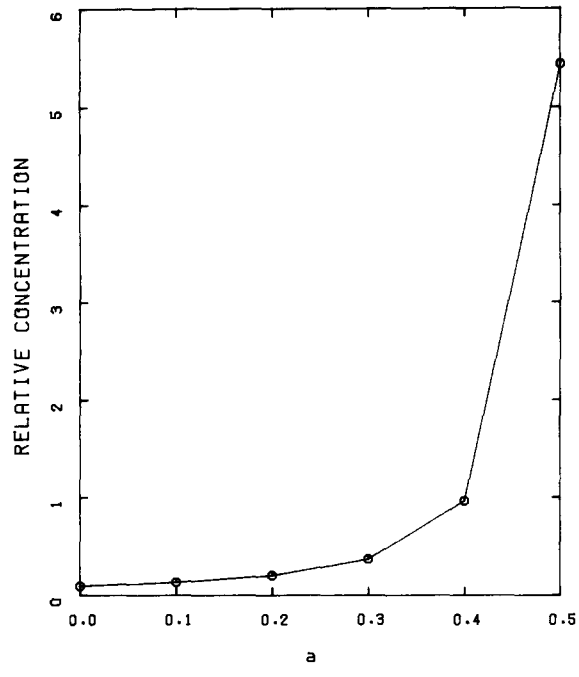

Figure 7 Concentration of polymer chain ends at sites along the wall but distant from any notch (such as Z in *Figure 6*) plotted as a function of a, the strength of the adsorption interaction. The concentrations displayed are relative to the concentration in the interior of the hexagon distant from any walls

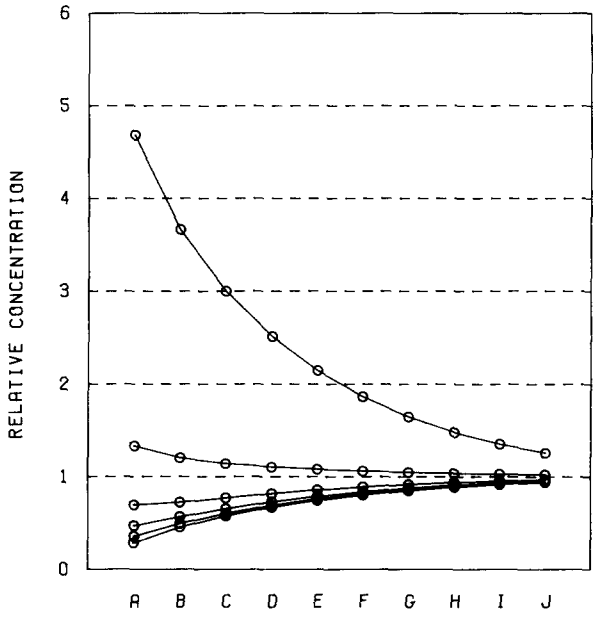

Figure 8 Concentration of polymer chain ends at the sites A, B, C, ..., (as in *Figure 6*), for various values of a, the strength of the adsorption interactions; a increases from 0 for the lowest curve to 0.5 for the highest curve in increments of 0.1. The displayed concentrations are relative to concentrations along the wall but distant from the notch (site Z)

the partition function of a chain distant from any boundaries. Therefore, *Figure 7* gives the concentration of chain ends near an infinite wall relative to the concentration distant from the wall. I show in Appendix 4 that the transition to adsorption, defined as the point at which $Q_\alpha = 6^N$, occurs at $a = \ln(3/2) \cong 0.41$. A transition near $a = 0.41$ is obvious in *Figure 7*. *Figure 8* displays the ratio of the partition functions for the sites labelled A, B, C, ... in *Figure 6* to the partition function for site Z. Therefore it represents the concentration of chain ends near the notch relative to the concentration near the wall but distant from the notch. It becomes clear from examination of *Figures 7* and *8* that in instances of weak attraction, $a < 0.41$, chains avoid the notch more strongly than they do the wall, while for $a > 0.41$, chains are preferentially adsorbed in the notch. I also see that the deference for the notch exhibited by chains with small a weakens as the attractive energy increases or the temperature decreases.

The chains in the calculation discussed above, with $N = 100$ and distant from any boundaries, have mean-square end-to-end distances of $100b^2$, for b the distance between nearest neighbour lattice sites. If I am to use these two-dimensional walks as models of three-dimensional polymers, I must consider them to be plane projections of random walks of mean-square end-to-end distance $150b^2$. If I let b be the distance between stems along the (110) direction of polyethylene crystals (4.55 Å) and assume a characteristic ratio of 6.7 (characteristic of polyethylene[19]) I calculate that these chains correspond to polyethylene chains of molecular weight 2700. Higher molecular weights are expected to exhibit the same trends as those given above, but I do expect a much more severe depletion of the sites near the notch on the depletion side of the adsorption transition.

I conclude that if no adsorption occurs, chains will make less contact with the boundaries near the notch than at sites distant from the notch, but with the frequency of contact increasing either with decreasing R_g (i.e., decreasing molecular weight) or increasing a (i.e., decreasing temperature). On the other hand, if adsorption does occur, chains will be attracted to the notch more strongly than to a flat wall.

APPENDIX 4

Position of the adsorption transition for the model of Appendix 3

Random walks in the lattice model considered above are six-choice walks. It follows that walks distant from any wall have partition functions of 6^N. I can compute the statistics of such walks near a flat attractive wall by applying transfer matrix techniques similar to those employed above. If I consider a flat wall much larger than the coil size of the chain, additional simplifications occur, since the transfer matrix need only carry information about steps between adjacent planes, not adjacent lattice sites. Therefore, elements of the transfer matrix may be defined so that

$$A_{\mu\nu} = 2 \exp[-(U_\mu + U_\nu)/2kT] \qquad (29)$$

if plane μ is accessible from plane ν in a single step, i.e., if $\mu = \nu$ or $\mu = \nu \pm 1$. $A_{\mu\nu}$ is zero for all other pairs of planes. The factor 2 results because for this particular walk, there are always two degenerate paths in the transition $\nu \rightarrow \mu$. I assume that μ and ν are any positive integers, U_μ is the energy accumulated by a lattice site visiting the μth plane. Therefore, $U_\mu = -akT$ if $\mu = 1$, otherwise U_μ is 0.

Therefore, if $x=e^{a/2}$, the transfer matrix may be written as

$$A=\begin{bmatrix} 2x^2 & 2x & & & & & \\ 2x & 2 & 2 & & & & \\ & 2 & 2 & 2 & & & \\ & & 2 & 2 & 2 & & \\ & & & 2 & 2 & 2 & \\ & & & & 2 & 2 & 2 \\ & & & & & & \ddots \end{bmatrix} \quad (30)$$

Chains near the wall will have partition functions equal to 6^N if the dominant eigenvalue of A is 6. Let us assume that the eigenvector corresponding to this eigenvalue is $[y\ z\ 1\ 1\ 1\ldots]$. The requirement that the eigenvalue be 6 yields the following equations:

$$\begin{aligned} 2x^2y+2xz&=6y \\ 2xy+2z+2&=6z \\ 2z+4&=6 \end{aligned} \quad (31)$$

These equations are satisfied when

$$x=(3/2)^{1/2},\ y=(2/3)^{1/2},\ z=1 \quad (32)$$

which occurs when $a=\ln(3/2)$. We conclude that the transition to adsorption occurs, for the present model, at $a=\ln(3/2)=0.41$.

APPENDIX 5

First contact between a Brownian particle and the walls of a square

In this appendix, I consider a Brownian particle initially at site $(L/2, L/2, 0)$ at $t=0$, which diffuses within a right rectangular tube bounded by the planes $x=0$, $x=L$, $y=0$, and $y=L$. I assume the particle migrates until it strikes one of the walls, and I ask for the probability distribution of the sites of first contact with the walls. In previous appendices, I have used the diffusion equation to model the conformational properties of ideal, Gaussian polymer chains, letting t represent the number of backbone bonds in the chain. Now, I employ the same formalism to treat the truly dynamic problem of Brownian trajectories with t representing actual time. I am considering the dynamics of polymers diffusing in solution over length scales much larger than the coil size, for which the coil can be thought of as a point-like particle. Therefore, I solve the diffusion equation, equation (1), subject to the boundary conditions $W=0$ at $x=0$, $x=L$, $y=0$, and $y=L$; $W=\delta(x-L/2)\delta(y-L/2)\ \delta(z)$ at $t=0$. For these boundary conditions, I can expand W in a Fourier expansion, retaining only the sine terms shown for the x and y dependence:

$$W=\sum_{m=1}^{\infty}\sum_{n=1}^{\infty}\int_{-\infty}^{\infty} dk\, F_{mn}(k)\sin\left(\frac{\pi m x}{L}\right)\sin\left(\frac{\pi n y}{L}\right)e^{ikz} \quad (33)$$

This equation yields to the usual techniques, I obtain for example:

$$F_{mn}(k)=(2/\pi L^2)\sin[\pi m/2]\sin[\pi n/2]\ e^{-Dtk^2} \times \exp\left[\frac{-Dt\pi^2}{L^2}(m^2+n^2)\right] \quad (34)$$

Note that only odd values of m and n contribute. I want to consider the following function of x:

$$\Phi(x)=D\int_0^{\infty} dt\int_{-\infty}^{+\infty} dz\left.\frac{\partial W}{\partial y}\right|_{y=0} \qquad (0\leqslant x\leqslant L) \quad (35)$$

The quantity

$$D\left.\frac{\partial W}{\partial y}\right|_{y=0}$$

is the probability density that the Brownian particle is absorbed in the surface element $dx\ dz$ during the time interval dt. Therefore $\Phi(x)$ gives the probability that the particle is absorbed in the interval $(x, x+dx)$ at any time and for all values of z, i.e., it is the probability distribution of the site of first contact with the wall. The derivative and the integrals appearing in equation (35) are all straightforward and I do not outline them here. With the aid of a tabulated series[18] I obtain:

$$\Phi(x)=L^{-1}\sum_{m=1}^{\infty}\frac{\sin[\pi m/2]}{\cosh[\pi m/2]}\ \sin(\pi m x/L) \quad (36)$$

The $m=3$ and higher terms in the above series only contribute about 1% to the sum, therefore

$$\Phi(x)\cong\sin\ (\pi x/L)/L\cosh\ (\pi/2) \quad (37)$$

which implies that

$$\Phi(x)\approx x \quad (38)$$

at small x.

APPENDIX 6

First contact between a Brownian particle and a rectangular notch

This appendix treats the same problem as Appendix 5, except for a different geometry. I initiate the Brownian particle at the site $(L, L, 0)$, and place absorbing boundaries at $y=0$ and $x=0$; i.e., I consider diffusion everywhere in the first quadrant. This problem is best treated by the method of images, in the same manner as in Appendix 1. I must place two sources at $(L, L, 0)$ and at $(-L, -L, 0)$, and two sinks at $(L, -L, 0)$ and $(-L, L, 0)$. I may write the following for W:

$$W=(4\pi Dt)^{-3/2}\textstyle\sum_i\omega_i\ \exp\left[\dfrac{-(\underset{\sim}{r}-\underset{\sim}{s}_i)^2}{4Dt}\right] \quad (39)$$

where

$$\omega_1=1 \quad \omega_2=-1 \quad \omega_3=1 \quad \omega_4=-1 \quad (40a)$$

$$\underset{\sim}{s}_1=(L,L,0) \quad \underset{\sim}{s}_2=(L,-L,0)$$

$$\underset{\sim}{s}_3=(-L,-L,0) \quad \underset{\sim}{s}_4=(-L,L,0) \quad (40b)$$

The analogue of equation (35) in this case is

$$\Phi(x)=D\int_0^{\infty} dt\int_{-\infty}^{+\infty} dz\left.\frac{\partial W}{\partial y}\right|_{y=0} \qquad (0\leqslant x) \quad (41)$$

Once again, the derivative and the integrals shown in equation (41) are straightforward. I obtain

$$\Phi(x)=(\pi L)^{-1}[(q^2-2q+2)^{-1}-(q^2+2q+2)^{-1}] \quad (42)$$

where

$$q=x/L \quad (43)$$

At small x this behaves as

$$\Phi(x) \approx x \tag{44}$$

just as in the previous case.

APPENDIX 7

First contact between a Brownian particle and a notch

I consider the same problem as Appendix 6, except that now the notch makes an arbitrary angle α, and I apply the notation and the coordinate system of Appendix 2. I initiate the walk at the point $(\rho, \theta, z) = (\rho_0, 0, 0)$. Therefore, for our purposes, we obtain W by setting $\theta_0 = 0$ in equation (6):

$$W = 4\alpha^{-1}\pi^{-1/2}(4Dt)^{-3/2} \exp[-(z^2+\rho^2+\rho_0^2)/4Dt] \times \sum_{n=1}^{\infty} I_s\left(\frac{2\rho\rho_0}{4Dt}\right)\sin\left(\frac{n\pi}{2}\right)\sin\left[\frac{n\pi}{\alpha}(\theta+\alpha/2)\right] \tag{45}$$

where $s = n\pi/\alpha$. The function representing the distribution of first contact sites is now written:

$$\Phi(\rho) = D\int_0^{+\infty} dt \int_{-\infty}^{+\infty} dz \frac{1}{\rho}\frac{\partial W}{\partial \theta}\bigg|_{\theta=-\alpha/2} \qquad (0 \leqslant \rho) \tag{46}$$

I have been unable to obtain an expression valid for arbitrary ρ, but I can make progress if I focus my attention on small ρ. At small ρ the Bessel function $I_s(x)$ obeys:

$$I_s(x) = (x/2)^s[\Gamma(s+1)]^{-1} \tag{47}$$

Performing the θ derivative and the z integral appearing in equation (46), and using equation (47) to represent the Bessel function yields:

$$\Phi(\rho) = \frac{\pi^{1/2}}{\rho\alpha^2}\sum_{n=1}^{\infty} n\left(\frac{\rho\rho_0}{4D}\right)^{n\pi/\alpha}\frac{\sin(n\pi/2)}{\Gamma(n\pi/\alpha+1)}\int_0^{\infty} dt \times t^{-(1+n\pi/\alpha)}\exp\left[\frac{-(\rho^2+\rho_0^2)}{4Dt}\right] \text{ (small } \rho) \tag{48}$$

The substitution $p = t^{-1}$ brings this into the form of equation (13). I finally obtain

$$\Phi(\rho) = \rho^{-1}\pi^{-1/2}\alpha^{-1}\sum_{n=1}^{\infty}\left(\frac{\rho\rho_0}{\rho^2+\rho_0^2}\right)^{n\pi/\alpha}\sin(n\pi/2) \tag{49}$$

Assuming $\rho \ll \rho_0$ and selecting the $n=1$ term only (valid for small enough ρ) yields:

$$\Phi(\rho) \approx \rho^{(\pi/\alpha-1)} \tag{50}$$

This agrees with the small x results of the last two appendices if I set $\alpha = \pi/2$, as expected. Interestingly enough, equation (50) also predicts the surface charge density generated on a wedge or notch by a line charge[21].

APPENDIX 8

Probability of first contact between a diffusing Brownian particle and a twin polymer crystal

In this appendix, I consider the diffusion of a Brownian particle in the domain pictured in *Figure 9*. I assume that at $t=0$ the Brownian particle lies somewhere on the perimeter of the outer square of side 20, and that it begins diffusing in the interior of the square. The walls of the square are reflecting boundaries. The particle is permitted to diffuse until making contact with the perimeter of the smaller polygon in the interior of the square. The smaller polygon represents, of course, the twin crystal. Since the domain is bounded, all Brownian particles will eventually strike the crystal. I seek the probability distribution of first contacts as a function of position on the perimeter of the crystal. *Figure 10* displays in more detail the assumed structure of the crystal. It has sides of length 1 and 2, as shown, and the interior angles shown. *Figure 10* also defines the coordinate ρ for this system, which specifies positions on the perimeter. ρ varies from 0 to 4, being 0 at the corner of the notch, 1 at either of the two horns, etc. onto 4 at the tip.

The distribution of first contact positions would be given formally by the solution of the diffusion equation,

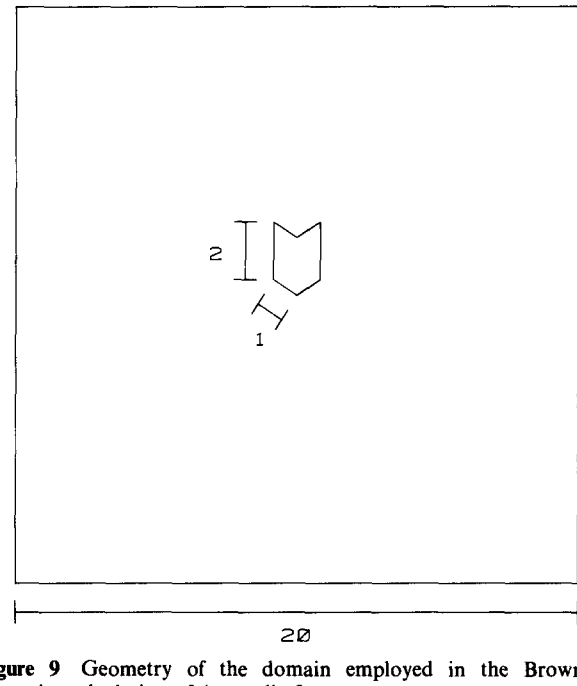

Figure 9 Geometry of the domain employed in the Brownian dynamics calculation of Appendix 8

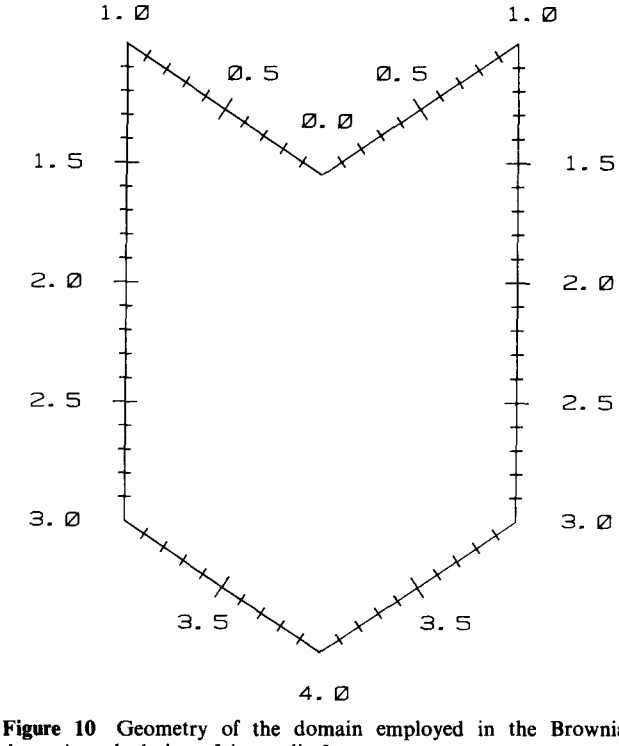

Figure 10 Geometry of the domain employed in the Brownian dynamics calculation of Appendix 8

just as in the last few appendices. However, the boundary value problem is undoubtedly too difficult to treat exactly and I therefore have examined the question by performing a Brownian dynamics simulation.

In a Brownian dynamics simulation, one begins at a particular point P_1 in phase space and, for a given time increment Δt, moves to a new point P_2 in such a way that the transition $P_1 \rightarrow P_2$ is representative of all possible transitions away from the point P_1 over the time interval Δt. In other words, one selects a new point P_2 in such a way that if the choice were made a large number of times, the new points P_2 would be distributed according to the distribution function expected at $t=\Delta t$ given that the distribution function was a Dirac δ function centred at P_1 at $t=0$. In the absence of any boundaries or external fields, the distribution function at $t=\Delta t$ is just a simple Gaussian. In the presence of boundaries, the distribution function is still Gaussian over times Δt small enough that the probability of actually reaching the boundary is negligible. I can make use of this fact in the present case by being careful always to choose a value of Δt small enough that the boundary would actually be reached with only a very small probability. Then in those infrequent cases where one actually does reach the boundary, I discard that particular step and try again. As the Brownian particle moves closer and closer to the boundary one takes smaller and smaller time steps, so that the boundary will, in fact, never be reached. Nevertheless, one still moves, after a large number of steps, arbitrarily close to the boundary. Therefore, I consider it a strike between the particle and the boundary once the particle has moved to within an arbitrary but small distance from the boundary. Also, in the present situation, one only needs to take progressively smaller time steps as we approach the perimeter of the crystal, not the perimeter of the outer square. Since the perimeter of the outer square is a reflecting boundary, I can treat excursions across this boundary by what amounts to the method of images. If, after any time step, the particle finds itself outside the outer square, move it back in by reflecting it through the walls of the square.

The following steps summarize the Brownian dynamics algorithm actually employed:

(1) Compute the minimum distance between the current position and the perimeter of the crystal. Call this d. Stop if $d<\varepsilon_1$ for ε_1 an arbitrarily chosen small number.

(2) Select a value Δt such that a Brownian particle in free space has negligible probability of moving a distance d or more. For two-dimensional diffusion, this can be the value of Δt which satisfies

$$\frac{1}{4\pi\Delta t}\int_d^\infty 2\pi r \exp\left[\frac{-r^2}{4\Delta t}\right] dr = \varepsilon_2 \qquad (51)$$

or

$$\Delta t = \frac{-d^2}{4(\ln \varepsilon_2)} \qquad (52)$$

for ε_2 an arbitrarily chosen small number.

(3) Given this value of Δt, select a displacement $\Delta r = (\Delta x, \Delta y)$ distributed according to the distribution function

$$\frac{1}{4\pi\Delta t}\exp\left[\frac{-(\Delta r)^2}{4\Delta t}\right] \qquad (53)$$

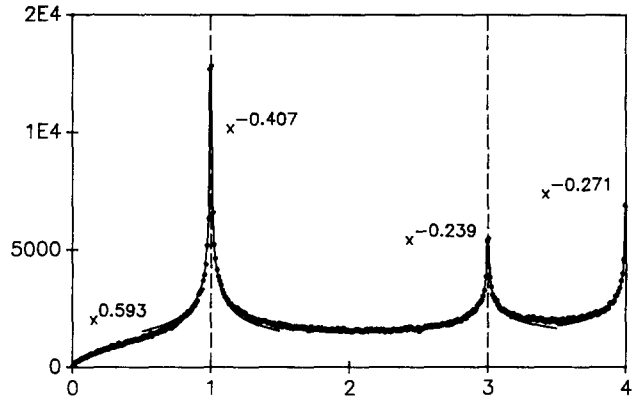

Figure 11 Number of Brownian particles arriving in the interval $(\rho-h/2,\ \rho+h/2)$ as a function of ρ for the Brownian dynamics calculation of Appendix 8

Then move to the new position $r+\Delta r$.

(4) If the new position lies outside the outer square, generate the actual new position by reflecting through the walls of the square.

(5) If the new point lies inside the crystal, reject this move, and go back to the previous position.

(6) Repeat steps 1 through 5 until the $d<\varepsilon_1$ criterion of step 1 is satisfied. When it is, record the value of ρ at which the particle meets the crystal, and initiate a new particle at the outer boundary.

Clearly, this approach will exactly simulate solutions to the diffusion equation only in the limit of vanishingly small ε_1 and ε_2. In practice, one faces a compromise since the computation time diverges as either ε_1 or ε_2 vanishes.

Figure 11 displays the function $\Phi(\rho)$ obtained by this approach, where $\Phi(\rho)d\rho$ is the probability that the Brownian particle is adsorbed on the crystal in the interval $(\rho,\ \rho+d\rho)$. *Figure 11* actually displays the integral of $\Phi(\rho)$ over an interval of width $h=0.01$, i.e., the fraction of particles arriving in the interval $(\rho-h/2,\ \rho+h/2)$. Near the singularities, such an integral is sufficiently different from $\Phi(\rho)$ times h that this distinction is necessary. Note that singularities occur at $\rho=1$, 3 and 4, and that a zero occurs at $\rho=0$. Based on the results of the last three appendices, I expect Φ to be proportional to ρ^{ν_0} for $\nu_0=(180/113)-1=0.5929$ near $\rho=0$; to $|\rho-1|^{\nu_1}$ for $\nu_1=(180/303.5)-1=-0.4069$ near $\rho=1$; to $|\rho-3|^{\nu_3}$ for $\nu_3=(180/236.5)-1=-0.2389$ near $\rho=3$; and to $|\rho-4|^{\nu_4}$ for $\nu_4=(180/247)-1=-0.2713$ near $\rho=4$. The simulation data prove to be consistent with these power laws.

Therefore, I conclude that Brownian particles diffusing onto the crystal from large distances make contact with a corner or notch with a probability density that depends on the distance d from the notch or corner according to the power law $d^{(\pi/\alpha-1)}$ for α the angle subtended by the notch or corner. For $\alpha<\pi$, the exponent is positive and the probability vanishes in the notch. If $\alpha=\pi/2$, the exponent is 1, in agreement with the results of Appendices 5 and 6. If $\alpha=\pi$, the exponent is zero, meaning that to lowest order in d, the probability density is uniform. If $\alpha>\pi$, the exponent is negative, implying that the probability density diverges. (However, the exponent $\pi/\alpha-1>-1$ always, so that the integral of the probability density remains finite.)